CHAPTER 2

Binuclear complexes with σ-bonded bis(oxamide) bridges.

2.1 Introduction

Derivatives of oxalic acid, oxamide and their anions like oxamate and oxamidate are being extensively studied since last two decades because of the versatile bonding mode that these ligands have with metal ions and the structural variations that can be brought about by functionalizing them.[1-2] The interest in these systems was routed in the observation of the efficient spin exchange interaction mediated by oxalate by Hendrickson and co-workers.[3] Later Kahn and co-workers[4] could tune the extent of spin exchange in the binuclear complexes of oxalate by capping the metal ions with variety of non bridging groups. Extensive studies have been carried out to reveal that oxamide bridges are the most suitable systems to design tunable molecular materials with extended structures having expected magnetic properties and possible biological applications.[5-7]

Oxamidate bridges are unique in the sense that (i) they can have easy *cis-trans* conformational change, which is important to afford symmetric or asymmetric oxamidate bridges.[8] (ii) they have extended π-delocalization which facilitates delocalization of spin and electron density over the paramagnetic centres, thus leading to strongly exchange coupled systems with modified and more often reversible redox. (iii) The oxamidato bridges are anionic yet π-bonding and hence they can stabilize the metal ions in higher oxidation states of transition metal ions.[9-10] This property is highly important as these systems can be potentially useful as catalytic oxidants and biologically significant as models for redox enzymes.[11-13] A very well known example is of the oxamide dianion $C_2O_2H_2N_2^{2-}$ [9,14a] and hydrazide groups[14b] in stabilizing copper(III) and nickel(III) metal ions[14a], and tetraaza pseudo-macrocyclic oxime and hydrazide ligands with adjustable cavity size.[14c] The design of binuclear or polynuclear complexes can be based on either functionalizing the oxamide, symmetrically or unsymmetricaly, on both nitrogen atoms i.e. the complexes can be based on N,N'-disubstituted oxamide frameworks, which contain oxamide bridging unit with two coordinating arms to occupy two or more coordination positions around each metal ion.[15-20] Another approach is based on joining two oxamide or oxamidate groups through an aliphatic or aromatic diamine. Both oxamide groups here have bridging ability; while the diamine brings the two oxamide parts close to form an additional, third, strongly coordinating tetradentate site. A variety of N,N'-disubstituted ligands and

other complexes have been reported.[21] These ligands undergo amide deprotonation at unusually lower pH (pH = 7-10) in presence of a metal ion like copper.[22-23] They can form *cis* mononuclear complexes under different pH conditions. The later are found to have strong exchange coupling between the copper centres. The *cis* mononuclear complexes can use the oxamide bridging mode to bind with second copper bound to a strong bidentate ligand like bipy, phen, or malonate.[24] It was shown that the extent of magnetic interaction in these complexes depends largely on the amine used in the synthesis of oxamide.[25] In order to synthesize complexes of different transition metal ions, it is necessary to match the ligand field by judiciously selecting an appropriate multidentate amine with oxygen, nitrogen or sulphur coordinating sites [26]. It was shown that nitrogen containing ligands in the N,N'-substituted oxamide are suitable to bind with copper(II) while, paramagnetic nickel(II) complexes are obtained with carboxylate containing amines in oxamides. A variety of aliphatic and aromatic diamines have been condensed with two equivalents of oxalyl chloride to form N,N'-bisoxamate ligands. The diamines used vary from en,[27a] 2pn[27b], 3pn[27c] to 1,2-diaminobenzene[9] and 1,8-diaminonaphthalene.[28] These ligands are capable of forming very stable mononuclear complexes with copper, where the amide protons remain dissociated. Thus N,N'-orthophenylene bis-oxamate and naphthalene-1,8-diylbisoxamate anions are capable of stabilising copper(II) as described earlier.[28] Similar bis-oxamides can form diamagnetic mononuclear complexes with nickel but in presence of copper, hydrolysis of end oxamide groups takes place leading to the formation of bisoxamate complex.[29] These mononuclear complexes are thought to be capable of using the amide oxygen coordinating sites to form oxamide bridged trinuclear complexes.

However, in majority of the cases the reactions ended up in the formation of polynuclear species.[30-32] Synthesis of trinuclear complexes with bis-oxamate ligands is possible only in presence of strong capping ligands like phen. Extensive studies have also shown that, the bidentate ligand used for capping also have very significant effect on the spin exchange.[31] Copper(II) complexes with bis-oxamate ligands have been reported with diamine, triamine e.g. tetramethylene diamine and pentamethyldiethylenetriamine or phen as capping ligands.[33] Complexes of bis-oxamide ligands with copper, remained so far unexplored probably due to the

possible copper catalysed hydrolysis of amide and the inability of end amide to form a bridge between two metal ions without deprotonation.

Here we report synthesis of binuclear complexes of three bis-oxamides, **oxen**, **ox2pn** and **ox3pn** from acidic solutions. The synthesis has been affected in presence of bipy and phen as capping ligands.

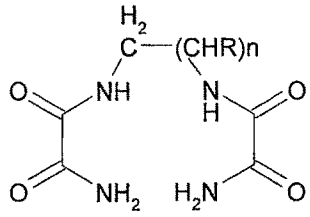

Fig.2.1

oxen, R = H, n = 1,

ox2pn, R = CH_3, n = 1,

ox3pn, R = H, n = 2.

Magnetic and electrochemical properties of the complexes have been studied with a view point of establishing structure property relationship.

2.2 Experimental

Materials

Ethyl oxamate, en, 2pn, 3pn, cupric acetate monohydrate (all AR) for synthesis and silver nitrate for cyclic voltammetric studies, were purchased from Merck. Methanol, DMF and DMSO used for UV-Vis spectroscopic analysis, conductivity measurements and voltammetric studies, were of AR or spectroscopic grade and purchased from Merck. Tetrabutyl ammonium perchlorate (TBAP, AR), used in voltammetric studies, was obtained from Fluka. All reagents were used as received and the solvents were distilled before use.

Synthesis of bis-oxamide Ligands

Synthesis of ligand oxen

4.680g (40mmol) of ethyl oxamate was suspended in 20ml of absolute ethanol and the suspension was heated to reflux. Most of the ethyl oxamate dissolved leaving a very light suspension. A solution of 1.224g (20.4mmol) of 1,2-

ethane diamine in 15ml absolute ethanol was added slowly and drop wise to the resulting hot solution. White crystalline product started separating. The addition was completed over 25 to 30min. The reaction mixture was allowed to reflux further for 4-5hrs for completion of reaction. The product **oxen** was filtered, washed with ethanol (5×5ml) and dried in air at ~ 60-70°C.

The ligands **ox2pn** and **ox3pn** have been synthesized using the above procedure with equivalent quantities of 1,2-propane diamine and 1,3-propane diamine in place of 1,2-ethane diamine.

General scheme of synthesis of ligands and complexes is presented in **Scheme 2.1**

Synthesis of Binuclear complexes

Synthesis of binuclear complex **$[(Cuphen)_2oxen]Cl_4$**

0.202g (1.0mmol) of **oxen** was placed in 30ml 50% aqueous ethanol in a 150ml flat bottom flask and stirred at RT. A 30ml 50% aqueous ethanol solution containing 0.598g (3.0mmol) of cupric acetate monohydrate, $Cu(CH_3COO)_2 \cdot H_2O$, and 0.396g (2.0mmol) of phen was added slowly with stirring to the ligand solution. The colour of the solution gradually changed to green during addition. Dilute hydrochloric acid solution (~6N, 50%) was added slowly and drop wise with constant stirring. The colour of the solution changed from dark green to very light green and a light green microcrystalline solid separated out at pH 1.5-2.0. The product **$[(Cuphen)_2oxen]Cl_4$ (2.1)** was filtered, washed with ethanol (10×5ml) and dried in air.

The procedure was repeated with equimolar quantities of phen, bipy and **ox2pn** and **ox3pn** in place of **oxen** to synthesize the complexes, **$(Cubipy)_2oxen]Cl_4$ (2.2)**, **$[(Cuphen)_2ox2pn]Cl_4$ (2.3)**, **$[(Cubipy)_2ox2pn]Cl_4$ (2.4)**, **$[(Cuphen)_2ox3pn]Cl_4$ (2.5)** and **$[(Cubipy)_2ox3pn]Cl_4$ (2.6)**, respectively.

Scheme 2.1

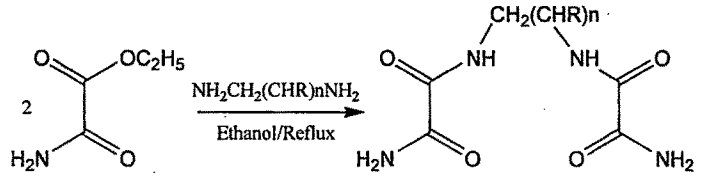

oxen, R = H, n = 1
ox2pn, R = CH_3, n = 1
ox3pn, R = H, n = 2

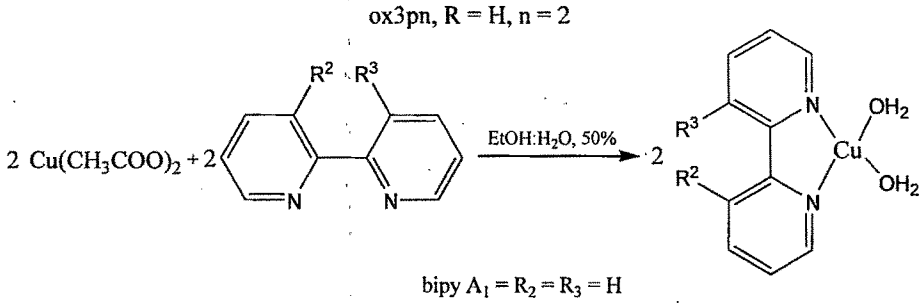

bipy $A_1 = R_2 = R_3 = H$
phen $A_2 = R_2 = R_3 = -CH=CH-$

dil.HCl

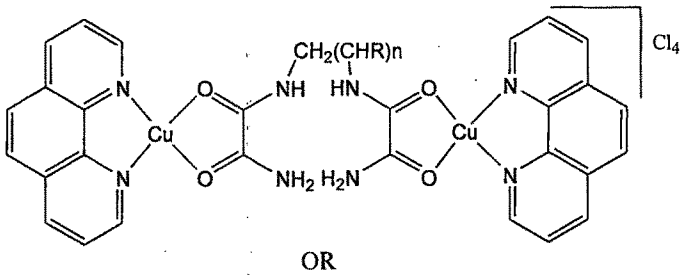

OR

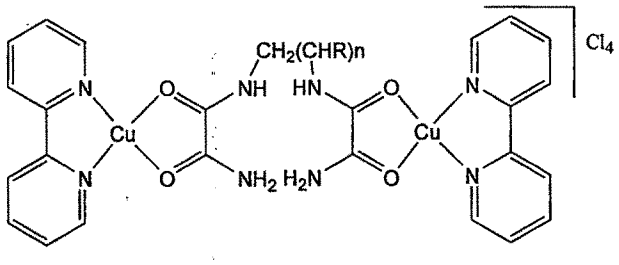

1, 2 : R = H, n = 1
3, 4 : R = CH_3, n = 1 and 2.1, 2.3, 2.5 A = phen
5, 6 : R = H, n = 2 2.2, 2.4, 2.6 A = bipy

Physical Measurements

The elemental analyses were carried out using Perkin-Elmer 2400 CHN/S Analyzer.

The electronic spectra of the complexes in the UV-VIS region were recorded in saturated methanolic solutions using Perkin-Elmer Lamda-35 recording spectrometer.

The IR spectra in the region 400-4000 cm^{-1} were recorded in the form of KBr pellets using Perkin-Elmer FTIR Spectrum RX1 spectrometer.

The FAB mass spectra were recorded on a JEOL SX 102/DA-6000 Mass Spectrometer Data system using Argon/xenon (6KV, 10mA) as FAB gas and m-nitro benzyl alcohol (NBA) as matrix.

The magnetic measurements were carried out from liq.N_2 to room temperature using an indigenous Faraday setup equipped with Mettler UMX-5 ultra micro balance and OMEGA-CYC3212 cryogenic temperature controller. The magnetic field of 0.8 Tesla was used.

Electrochemical properties were studied by cyclic voltammetric experiments using PAR Model 174A polarographic analyzer, PAR Model 175 Universal programmer and PAR Model 303A electrode system. Pt disk working electrode, Pt wire counter electrode and $Ag/AgNO_3$ (0.1M in CH_3CN) as reference electrodes were used. The voltammograms were recorded in DMSO solutions using 0.1M tetrabutyl ammonium perchlorate (TBAP) as electrolyte. All potentials are referred to Cp_2Fe/Cp_2Fe^+ couple.

2.3 Results and Discussion

Characterization of dioxamide ligands

The elemental analyses of all the three synthesized dioxamide ligands (Table 2.1) were found within the appreciable range. ^1H NMR spectra were recorded using D_6-DMSO-$CDCl_3$ mixed solvents and was found to be matching with the proposed structures.

Table 2.1 The yields, physical constants and elemental analysis of the ligands.

Ligand	Yield (%)	Melting Point (°C)	Elemental Analysis (%)		
			C	H	N
oxen	63	272 (dec.)	35.96	5.13	28.21
$C_6H_{10}O_4N_4$			(35.64)	(4.95)	(27.72)
ox2pn	52	257(dec.)	39.34	5.75	25.47
$C_7H_{12}O_4N_4$			(38.88)	(5.55)	(25.92)
ox3pn	59	277(dec.)	39.11	5.87	25.52
$C_7H_{12}O_4N_4$			(38.88)	(5.55)	(25.92)

^{1}H NMR analysis of the ligands

The ^{1}H NMR spectra of the three oxamide ligands in mixed D_6-DMSO-$CDCl_3$ solvents.

In the ^{1}H NMR spectrum of, **oxen**, (**Fig.2.2**) a quartet corresponding to both pairs of $-CH_2-$ protons (c) at (3.2ppm, 4H) has been observed. Both –NH (b) protons show triplet at (8.78ppm, 2H) and one proton from each $-NH_2$ (a) shows singlet at (7.75ppm, 2H) and another singlet at (8.03ppm, 2H).

In the ^{1}H NMR of **ox2pn**, **(Fig.2.3)** a doublet corresponding to $-CH_3$ (f) has been observed at 1.0ppm, corresponding to 3H. A triplet corresponding to 2 protons in $-CH_2-$ (d) at 3.2ppm and a septet corresponding to 1H in -C-H (e) at 3.9ppm have been observed. The two sets of terminal $-NH_2$ protons are non equivalent and appear in the ^{1}H NMR as two singlets at 7.8ppm (2H) and 8.1ppm (2H), respectively. The secondary amide protons are also non equivalent. The –N-H (c) proton appears as a doublet at 8.65ppm (1H), while the –N-H (b) proton appears as a triplet at 8.8ppm (1H).

Ligand **ox3pn**, **(Fig.2.4)** has C_2 symmetric structure. A quintet corresponding to the central $-CH_2$ (d) (2H) was observed at 1.6ppm. Both $-CH_2$ (c) show quartet at 3.1ppm, corresponding to a total of four protons. Both $-NH_2$ (a) show two singlets at 7.75ppm, corresponding to two protons and at 8.05ppm, for two protons. A triplet has been observed corresponding to two protons in -N-H (b) at 8.75ppm.

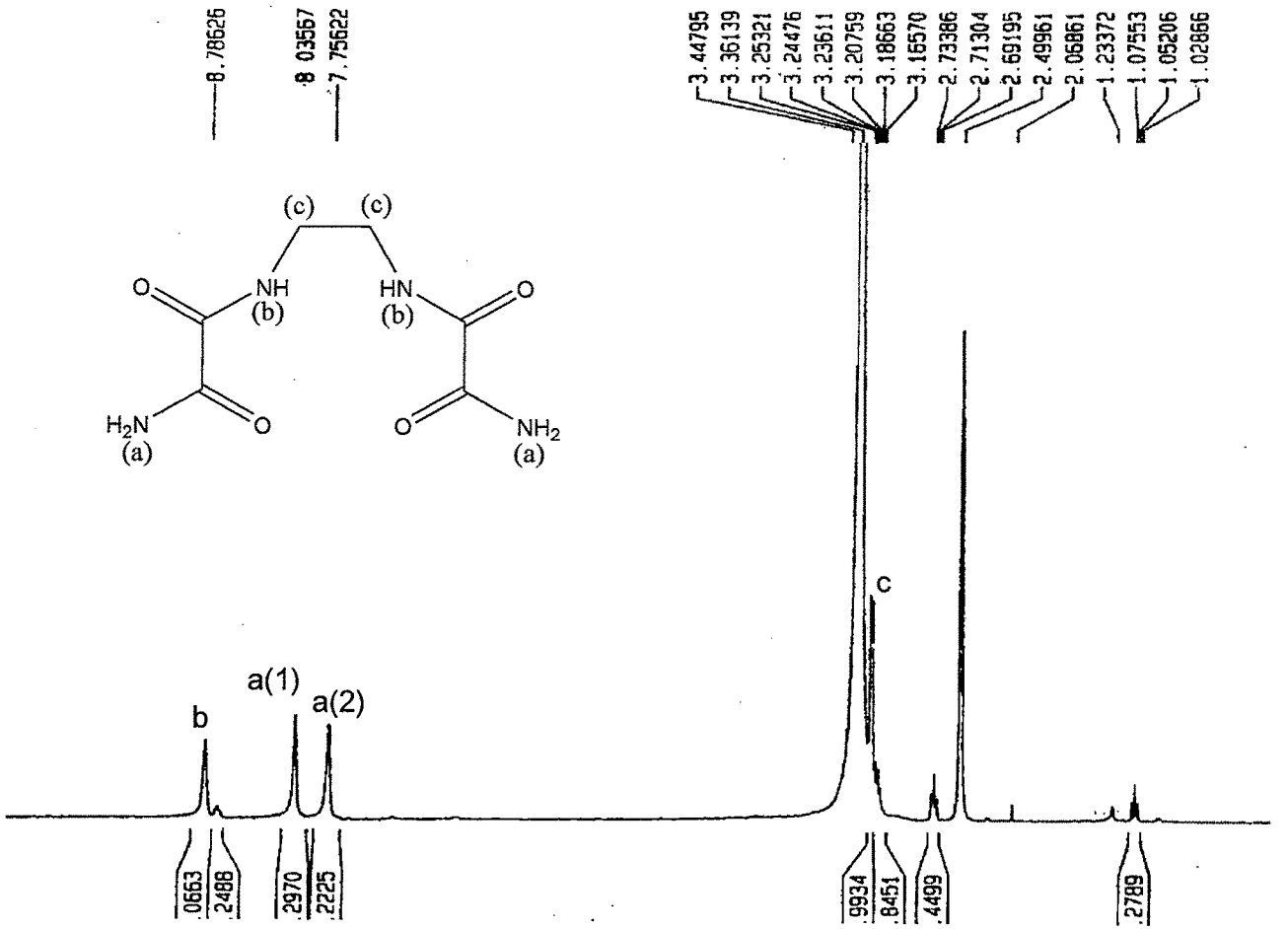

Fig. 2.2 ^{1}H NMR spectrum of ligand **oxen.**

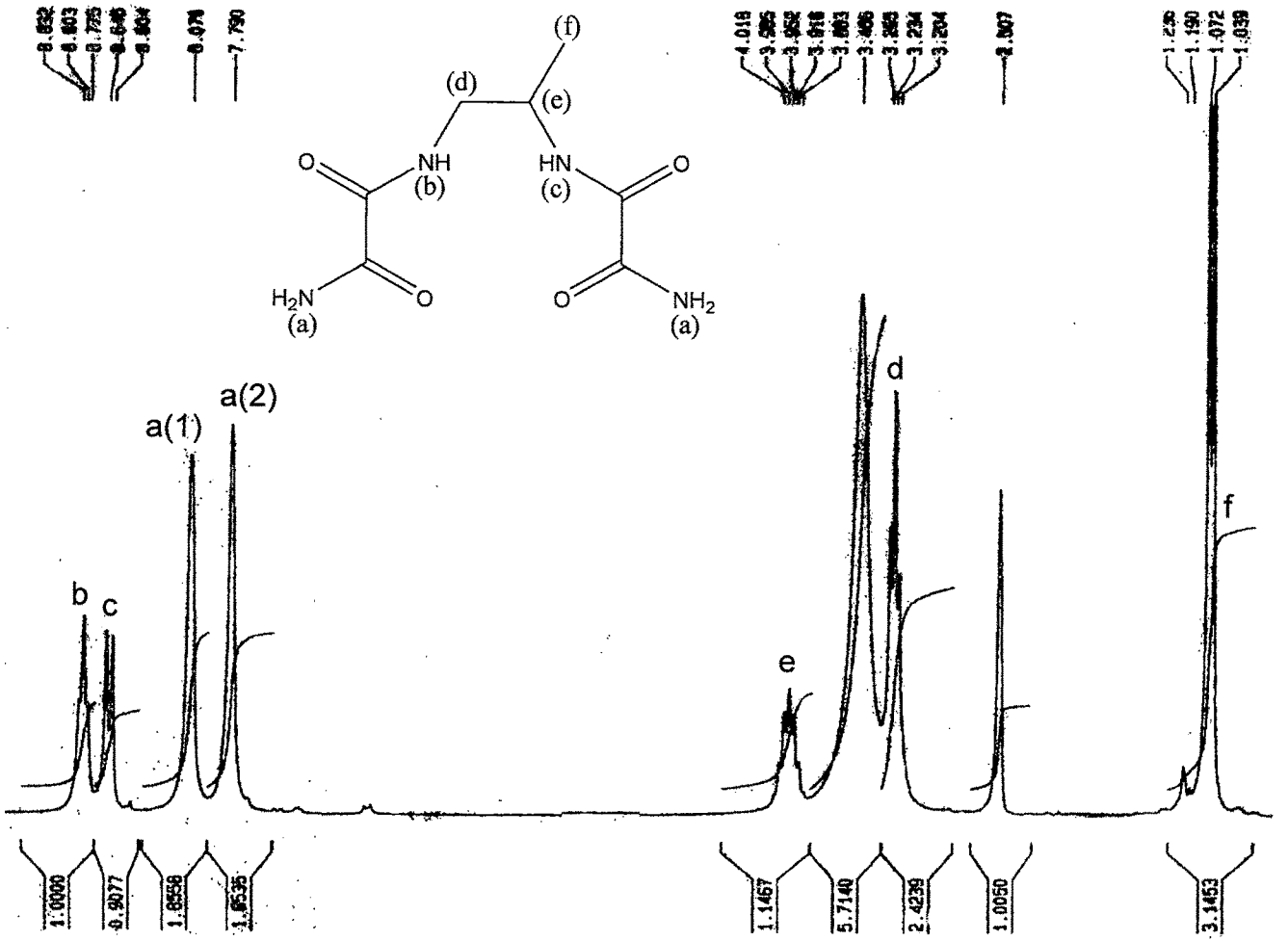

Fig. 2.3 ^{1}H NMR spectrum of ligand **ox2pn.**

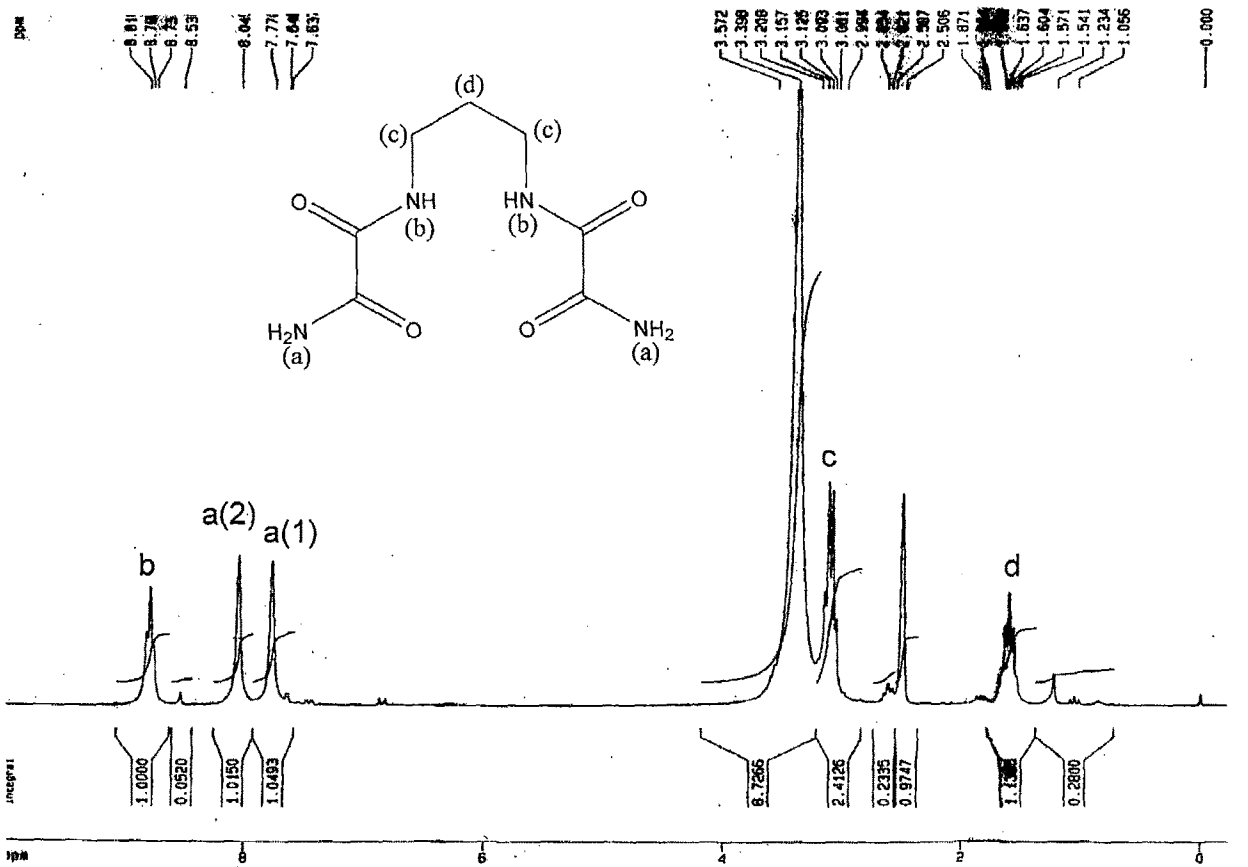

Fig. 2.4 ^{1}H NMR spectrum of ligand **ox3pn.**

In the ^{1}H NMR spectrum of the ligands **oxen**, **ox2pn** and **ox3pn**, one of the proton of each $-NH_2$ is deshielded and appears at higher ppm values. This could be justified on the basis of hydrogen bonding. One of the hydrogen from both $-NH_2$ groups, forms a hydrogen bond with the adjacent carbonyl oxygen. The structures of the ligands (**Fig.2.13** to **2.15**) optimized by *ab initio* quantum mechanical calculations using 6-31G basis set also show the presence of H-bonding which results in different chemical shift values corresponding to the two –N-H protons. Thus the ^{1}H NMR of all the three ligands confirms their formation.

Characterization of complexes

The bis-oxamide ligands reported here are expected to possess both bi- and trinucleating ability. Repeated attempts to synthesize the binuclear or trinuclear complexes at natural pH of the solution obtained by mixing the reagents were unsuccessful. Under these conditions, the bis oxamide ligands deprotonate to form the thermodynamically stable, neutral, mononuclear complexes where the Cu^{2+} ion occupies the central, tetra dentate coordination site. These mononuclear complexes could be very easily isolated and the formation of the complexes was confirmed by various analytical methods.

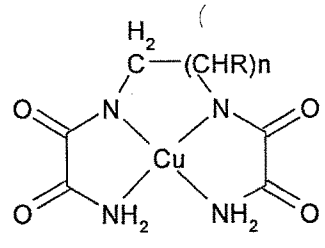

Fig. 2.5 Mononuclear complex of the oxamide ligands.

The elemental analyses (Table 2.2) of these mononuclear complexes were found to be in the appreciable range.

The synthesis of above type of mononuclear complexes was attempted earlier.[34,35] It was observed that **oxen** can form a copper(II) complex with both 2° amide N-H deprtonated. However, the attempt to synthesize similar complex with **ox3pn** was unsuccessful resulting in hydrolysis of end amide groups. Our attempt to synthesize trinuclear complexes at natural pH of the solution (~5.5) resulted in the formation of the

above mononuclear complexes as the presence of copper(II) can facilitate the amide deprotonation as observed earlier at several instances. Study of the pH dependence of the species formed by an N,N'-disubstituted oxamide[36,37] has shown that the free ligand undergoes amide deprotonation between pH 12-13 while in presence of copper(II) and nickel(II) the deprotonation occurs between pH 3-5 and 7-9, respectively.

Table 2.2 Elemental analysis of the mononuclear complexes.

Complex	Yield	Elemental Analysis (%)			
	(%)	C	H	N	Cu*
[Cuoxen]	78	27.42	3.45	20.77	24.57
$C_6H_8O_4N_4Cu$		(27.320)	(3.035)	(21.249)	(24.110)
[Cuox2pn]	69	30.455	4.003	19.897	23.312
$C_7H_{10}O_4N_4Cu$		(30.265)	(3.603)	(20.177)	(22.894)
[Cuox3pn]	71	30.155	4.053	20.057	23.126
$C_7H_{10}O_4N_4$ Cu		(30.265)	(3.603)	(20.177)	(22.894)

*Estimation of Copper was done by gravimetric analysis.

It has been very well proved in case of peptides[38-39] that in presence of a metal ion, thermodynamically more stable complexes with higher denticity of ligand can be formed by amide deprotonation. Also, a number of diamides form complexes through deprotonated amide nitrogen under ambient conditions. The present case is expected to be very similar. For an obvious reason, neutral diamide coordination should take place at lower pH values. It is also known that the heterocyclic N bases viz. bipy and phen can form highly stable ternary complexes with oxygen donors.[40] Hence, it was decided to carry out the reactions in acidic media. In all the cases reported here, the binuclear complexes formed at pH 1.5-2, whereas accommodating a third metal ion at the central site of the ligands was not possible at these pH values.

All the six binuclear complexes formed with yields between 45-76%. The elemental analysis is in good accordance with the values calculated from the formulae suggested in Table 2.3.

Table 2.3 Yields, Analytical data and Molar conductivity of the Complexes.

Sr. No.	Complex	Yield (%)	Elemental Analysis (%)*			Molar Conductivity $\Omega^{-1}cm^{-1}mol^{-1}$
			C	H	N	
1	**[(Cuphen)$_2$oxen]Cl$_4$** $C_{30}H_{26}O_4N_8Cu_2Cl_4$	60.67	43.50 (43.31)	3.25 (3.12)	13.96 (13.47)	55
2	**[(Cubipy)$_2$oxen]Cl$_4$** $C_{26}H_{26}O_4N_8Cu_2Cl_4$	44.51	39.80 (39.84)	3.55 (3.32)	14.79 (14.30)	45
3	**[(Cuphen)$_2$ox2pn]Cl$_4$** $C_{31}H_{28}O_4N_8Cu_2Cl_4$	76.05	44.34 (44.01)	3.08 (3.31)	12.99 (13.25)	45
4	**[(Cubipy)$_2$ox2pn]Cl$_4$** $C_{27}H_{28}O_4N_8Cu_2Cl_4$	70.84	41.12 (40.64)	3.58 (3.51)	14.55 (14.05)	45
5	**[(Cuphen)$_2$ox3pn]Cl$_4$** $C_{31}H_{28}O_4N_8Cu_2Cl_4$	63.58	44.36 (44.01)	3.34 (3.31)	13.48 (13.25)	45
6	**[(Cubipy)$_2$ox3pn]Cl$_4$** $C_{27}H_{28}O_4N_8Cu_2Cl_4$	67.79	41.00 (40.64)	3.30 (3.51)	14.50 (14.05)	45

*The values in parentheses are calculated for the empirical formulae in column 2.

Conductivity measurements

Molar conductivity values of all complexes were found to be between 45-55 $\Omega^{-1}cm^2mol^{-1}$ in the (1×10^{-3}M) DMF solutions. This indicates that, the chloride ions, though weakly, are coordinated to copper(II) ions.

FAB Mass spectral studies

FAB-Mass spectra of two representative binuclear complexes **[(Cuphen)$_2$ox2pn]Cl$_4$** and **[(Cubipy)$_2$ox2pn]Cl$_4$** were recorded. The chloride coordination with a metal ion is usually very weak and hence the abundance of species involving chloride binding can be usually very low.

In complex **[(Cuphen)$_2$ox2pn]Cl$_4$**, (**Fig.2.7**), a peak corresponding to **[(Cuphen)$_2$ox2pn]Cl$_4$+H$^+$** confirms the binuclear complex formation. The other peaks corresponding to fragments like **[(Cuphen)$_2$ox2pn]$^{4+}$/4** in complex **[(Cuphen)$_2$ox2pn]Cl$_4$** and **[(Cubipy)$_2$ox2pn]Cl$_3^+$**, **[(Cubipy)$_2$ox2pn]$^{4+}$** in complex

[(Cubipy)$_2$ox2pn]Cl$_4$ confirm the formation of binuclear complexes as per the suggested formulae. A peak corresponding to the metal containing species and **ox2pn**, **[Cuox2pn]** in both the complexes indicate the presence of the ligand as well as copper. Other significant fragments observed in the mass spectra are tabulated below in Table 2.5 and Table 2.6. The corresponding fragments are presented in **Fig.2.9** and **Fig.2.10.**

Table 2.4 Fragments observed in the FAB-Mass spectrum of the complex **[(Cuphen)$_2$ox2pn]Cl$_4$** in m-nitrobenzyl alcohol.

Description of species	Calculated (m/Z)	Observed (m/Z)
[CuPhen]$^+$	243	243
[(Cuphen)$_2$ox2pn]Cl^{3+}/3	245	245
[(Cuphen)$_2$ox2pn]Cl$_4$+2H$^+$/2	422	422
[Hox2pn]$^+$	217	217
[cuox2pn-2H]$^+$	277	277
[Cu$_2$ox2pn-2H]$^+$	340	340
[(Cuphen)$_2$ox2pn]Cl$_2^{2+}$/2	386	386
[(Cuphen)$_2$ox2pn]$^{4+}$ / 4	175.75	176
[Phen+H]$^+$	181	181
[(CuPhen)$_2$ox2pn]Cl$_4$.H$_2$O+H$^+$	865	864
[[Cuphen)2ox2pn]$^{4+}$ + 4Cu]	956	955

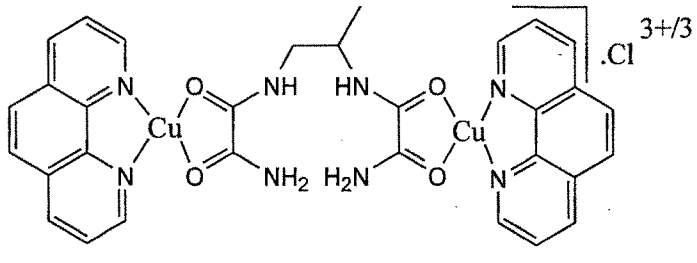

observed at m/Z = 245.

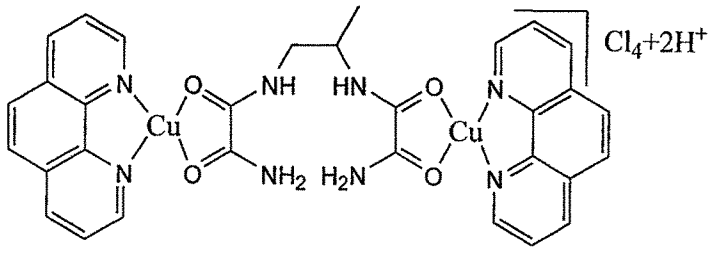

observed at m/Z = 422.

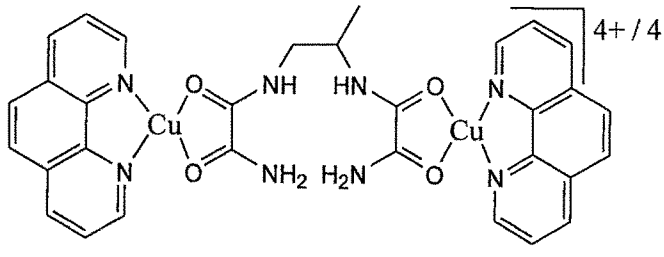

observed at m/Z = 176.

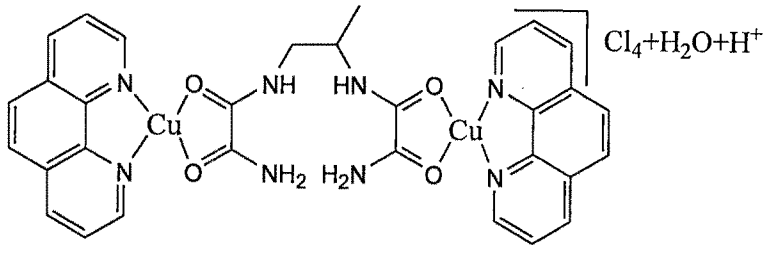

observed at m/Z = 864.

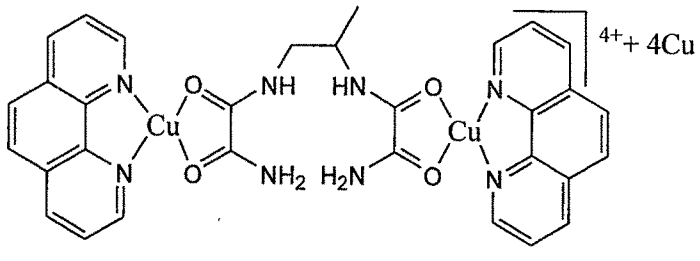

observed at m/Z = 955.

Fig.2.6 Species/ fragments of complex **[(Cuphen)$_2$ox2pn]Cl$_4$** in FAB-Mass.

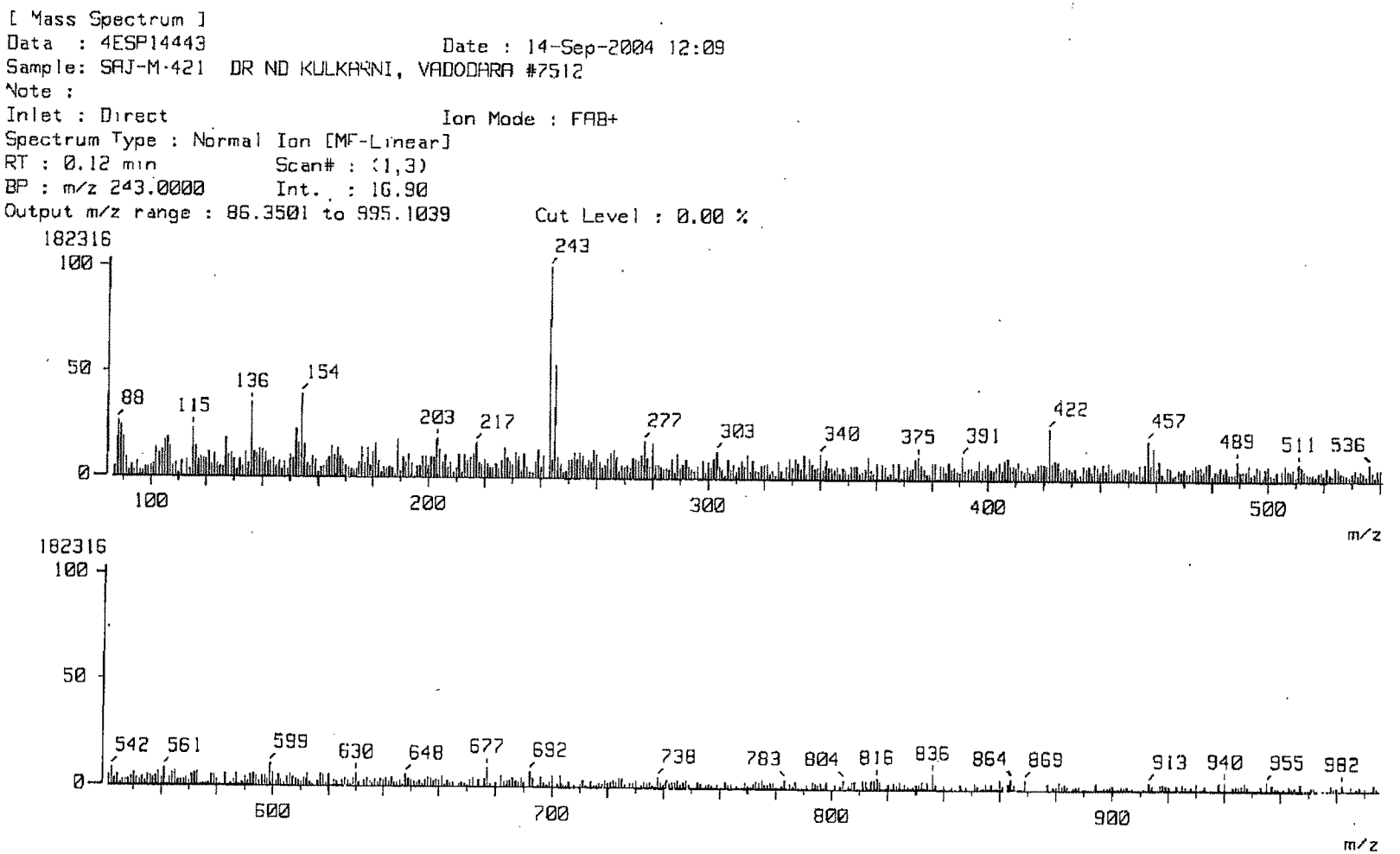

Fig 2.7 FAB-Mass spectrum of complex **[(Cuphen)$_2$ox2pn]Cl$_4$**

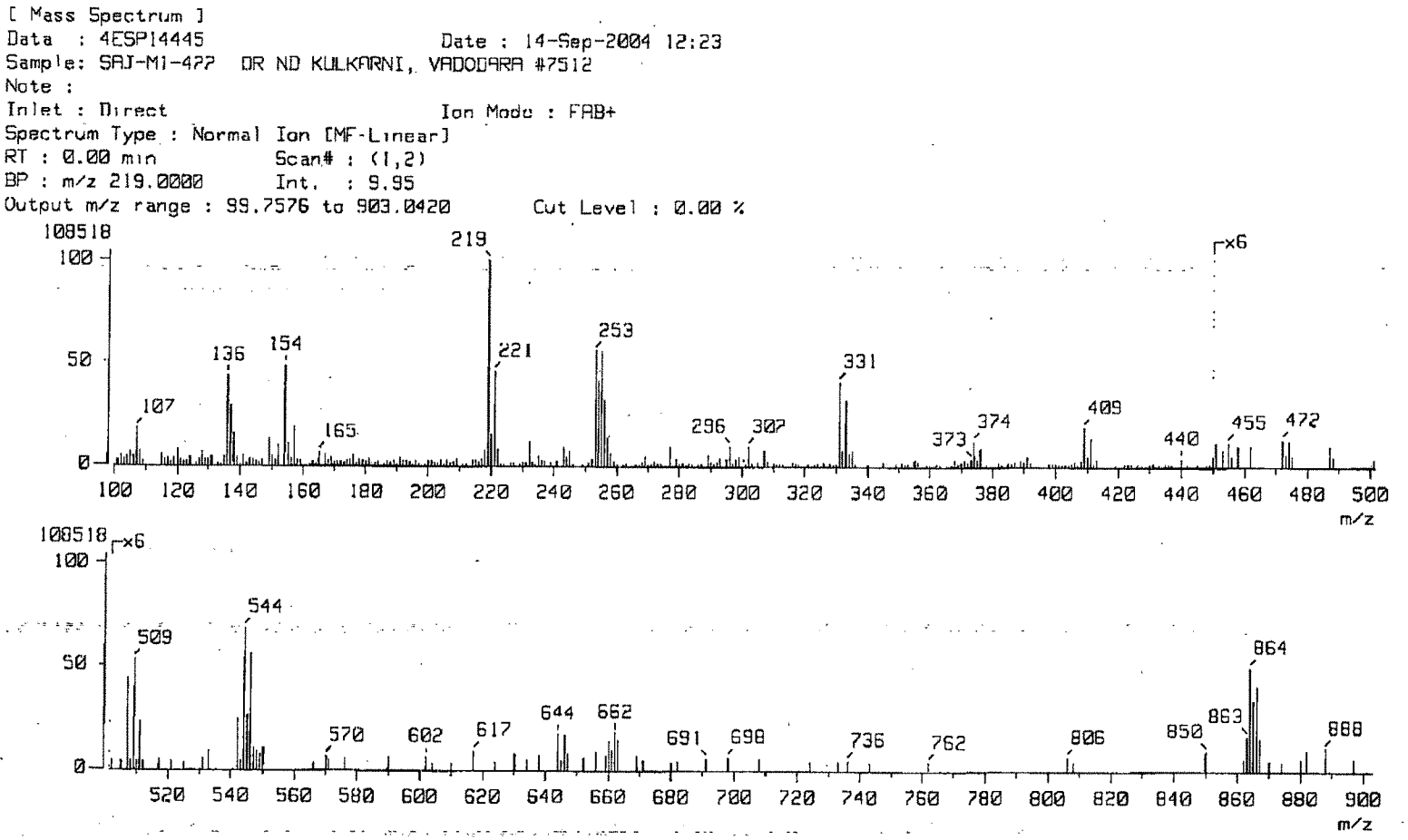

Fig.2.8 FAB-Mass spectrum of complex **[(Cubipy)$_2$ox2pn]Cl$_4$**.

Table 2.5 Fragments observed in FAB mass of complex **$[(Cubipy)_2ox2pn]Cl_4$** in m-nitrobenzyl alcohol.

Description of species	Calculated (m/Z)	Observed (m/Z)
$[Cubipy]^+$	219	219
$[(Cubipy)_2ox2pn]^{4+}$-$2H^+$/2	331	331
$[Cubipyox2pn]Cl_2+H^+$	506	507
$[Cubipyox2pn]Cl_2^+$+$3H_2O$	545	544
$[Cu_2ox2pn]Cl_2^+$	412	411
$[Cuox2pnbipy]Cl^+$	472	472
$[(ox2pn\text{-}H)_2]+H^+$	108	107
$[ox2pn.H_2O]^+$	234	232
$[(Cubipy)_2ox2pn]^{4+}$/4	165	165
$[(Cubipy)_2ox2pn]Cl_3^+$	761.5	762
$[[(Cubipy)_2ox2pn]Cl_2\text{-}H]^+$	724	724
$[Cuox2pn\text{-}2H]^+$	277	277
$[Cuox2pnbipyH_2O]^+$	453	453
$[Cu(bipy)_2^{2+}\text{-}H]^+$	374	374
$[bipy+H]^+$	157	157
$[Cu_2ox2pnbipy]Cl_2$	570	570
$[(Cubipy)_2ox2pn]Cl_4$+Cu	860.62	864

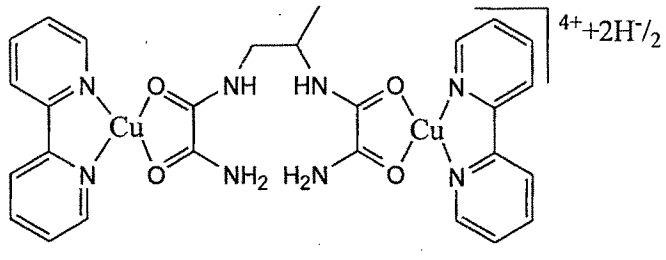

observed at m/Z = 331.

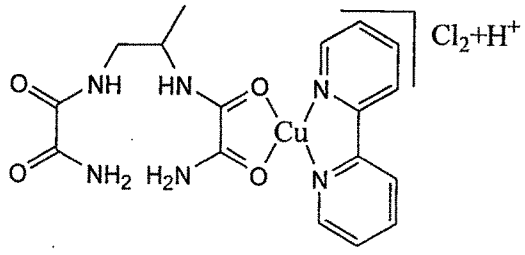

observed at m/Z = 507.

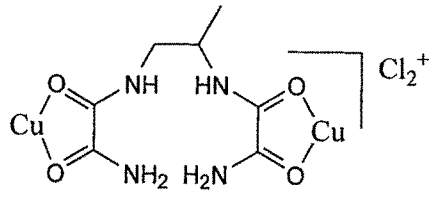

observed at m/Z = 411.

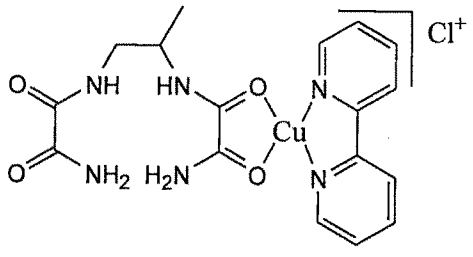

observed at m/Z = 472.

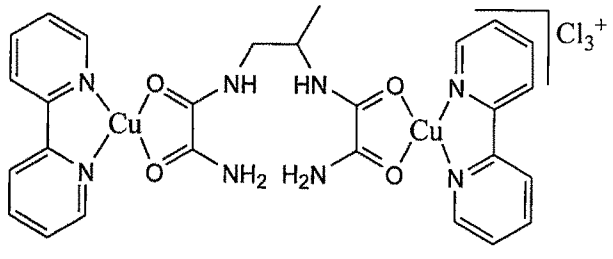

observed at m/Z = 762.

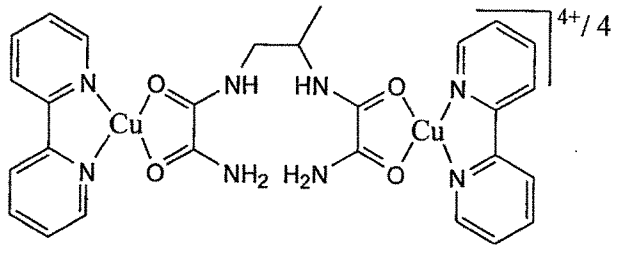

observed at m/z = 165.

Fig.2.9 Species/ fragments of complex **[(Cubipy)$_2$ox2pn]Cl$_4$** in FAB mass.

Electronic and Infrared Spectral Studies

The absorptions observed in the electronic spectra of the complexes in saturated methanolic solutions are listed in Table 2.6.

The electronic spectra of the complexes in methanolic solutions exhibit intraligand transitions in 200-350nm region. The characteristic π-π^* transitions corresponding to phen are observed at 272nm in complex **[(Cuphen)$_2$oxen]Cl$_4$**, **[(Cuphen)$_2$ox2pn]Cl$_4$** and **[(Cuphen)$_2$ox3pn]Cl$_4$**. Other features of phen are also observed. The π-π^* transitions characteristic of bipy are observed at 300nm in the complexes **[(Cubipy)$_2$oxen]Cl$_4$**, **[(Cubipy)$_2$ox2pn]Cl$_4$** and **[(Cubipy)$_2$ox3pn]Cl$_4$**. The characteristic transitions in coordinated phen and bipy have been observed at 326 and 344nm in complexes containing phen as the terminal ligand and at 322 and 327nm in the complexes having bipy as a terminal ligand. Weak and broad bands corresponding to the ligand field transitions are observed between 715-720nm. The absorption at longer wavelengths in spite of the presence of strongly coordinating bipy or phen indicates that the geometry of the complexes must be distorted from regular square planar geometry.

Table 2.6 Transitions observed in the Electronic absorption spectra of the complexes.

Complex	Intra Ligand Transitions λ (nm)	Ligand Field Transitions λ (nm)
[(Cuphen)$_2$oxen]Cl$_4$	205.11, 225, 244.34, 272.61, 295,326,344.	719.0
[(Cubipy)$_2$oxen]Cl$_4$	203.38, 244, 268.84,300.06, 310, 322.9, 327.7	715.02
[(Cuphen)$_2$ox2pn]Cl$_4$	204.91,225, 244.00, 272.5, 295,326,344.	718.96
[(Cubipy)$_2$ox2pn]Cl$_4$	203.32, 244, 268.6, 300.1, 310,322.9, 327.7	715.94
[(Cuphen)$_2$ox3pn]Cl$_4$	204.64, 225, 244.25, 272.51, 295,326,344	716.92
[(Cubipy)$_2$ox3pn]Cl$_4$	203.71, 244, 268.94,300.09, 310, 322.9, 327.7	716.06

Some important absorptions in the IR spectra of the complexes are listed in Table 2.7. The absorption due to >C=O stretching frequency, has been observed at 1656 in **oxen**, at 1660 in **ox2pn** and at 1651cm^{-1} in **ox3pn**. These frequencies are not much

affected after coordination with the metal ion. The band due to aliphatic -C-N- vibration at 1112 in **oxen**, at 1145cm^{-1} in **ox2pn** and at 1103cm^{-1} in **ox3pn** have been found to split in their complexes. Absorption corresponding to the stretching frequencies of primary amide >N-H, have been found at 3382 in **oxen**, at 3385 in **ox2pn** and at 3388cm^{-1} in **ox3pn.** These are not much affected after the coordination. >N-H streching in secondary amide was observed at 3315 in **oxen**, at 3309 in **ox2pn** and at 3319cm^{-1} in **ox3pn.** These are also not much affected after the coordination. Aliphatic C-N vibration in **oxen** at 1413, in **ox2pn** at 1411 and in **ox3pn** at 1411cm^{-1} showed increased intensity with a small shift in the complexes. The alkyl –C-H streching in the ligand **oxen** is observed at 2956cm^{-1}, at 2936 and 2980 in **ox2pn** and at 2951cm^{-1} in **ox3pn,** whereas the –C-H bending (in $-CH_2$) is observed at 1451, 1457 and at 1461cm^{-1}, respectively. These remain unaffected in the complexes. Very small shifts in the $\nu_{C=O}$ and ν_{N-H} are indicative of the coordination of the oxamide ligand with copper through amide oxygen atoms and not through nitrogen.

Table 2.7 FTIR frequencies of ligands and complexes.

Important Freq. (cm^{-1})	>C=O	ν N-H (1^0amide) (free)	ν N-H (2^0amide) (bonded)	δ N-H (2^0amide) (bending)
oxen	1656	3382	3315	1548
ox2pn	1660	3385	3309	1543
ox3pn	1651	3388	3319	1549
[(Cuphen)$_2$oxen]Cl$_4$	1654	3381	3313	1549
[(Cubipy)$_2$oxen]Cl$_4$	1655	3381	3313	1548
[(Cuphen)$_2$ox2pn]Cl$_4$	1658	3384	3307	1543
[(Cubipy)$_2$ox2pn]Cl$_4$	1660	3383	3306	1544
[(Cuphen)$_2$ox3pn]Cl$_4$	1656	3383	3312	1545
[(Cubipy)$_2$ox3pn]Cl$_4$	1654	3383	3311	1545

All the peaks corresponding to coordinating groups in ligands do not show any major changes in their frequencies after complexation. It has been shown[41] that in the case of an oxamide dianion coordinated to two metal ions as a bridging ligand, the amide I band

reverts to near its original position between 3382 - 3389cm^{-1} as in the protonated species. Similar observation is made in the present complexes, confirming the oxamide bridging between the two copper ions.

The presence of absorption bands at 721, 736 and 855cm^{-1} confirms the presence of phen in complexes **[(Cuphen)$_2$oxen]Cl$_4$**, **[(Cuphen)$_2$ox2pn]Cl$_4$** and **[(Cuphen)$_2$ox3pn]Cl$_4$** and peaks corresponding to bipy at 730 and 777cm^{-1} confirm the presence of bipy in complexes **[(Cubipy)$_2$oxen]Cl$_4$**, **[(Cubipy)$_2$ox2pn]Cl$_4$** and **[(Cubipy)$_2$ox3pn]Cl$_4$** and hence confirm the complex formation and coordination of the phen and bipy in the respective complexes. Thus the IR spectra of the complexes are combinations of the infrared spectra of the oxalodiamide and tertiary diamine ligands and comprise of all important features of both. The important peaks corresponding to the stretching of amide >C=O and primary and secondary amide N-H appear in the same region as the free ligands with very small shifts towards lower energy. The small shifts are due to the coordination of dioxamide ligands with metal ion through oxygen atoms without appreciable change in electron density distribution within oxamide. The coordination through nitrogen would have resulted in very large shifts in the $\nu_{>C=O}$ towards lower energy. The oxygen coordination is further supported by ESR.

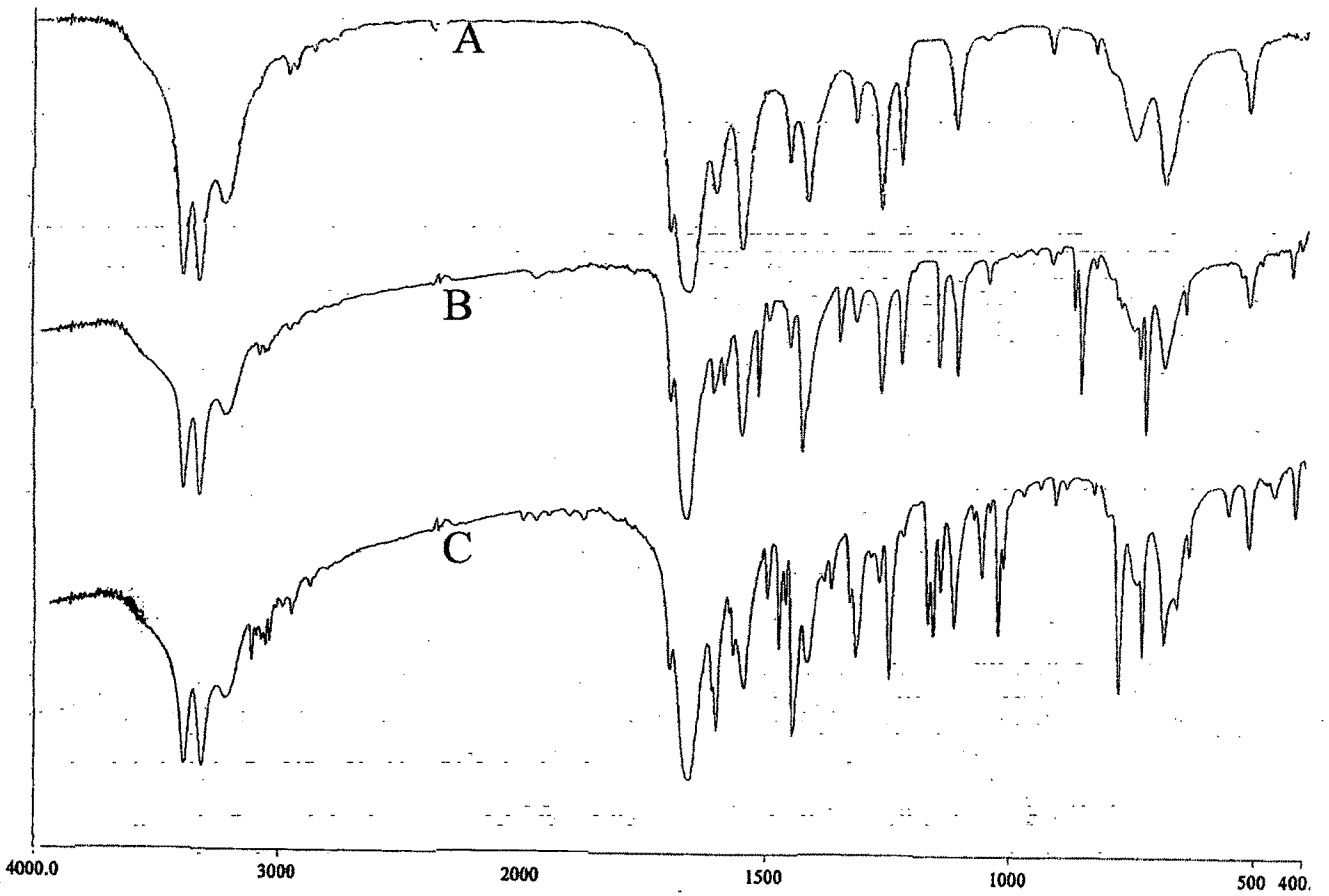

Fig.2.10 FTIR spectrum of ligand **oxen** (A), complex **[(Cuphen)$_2$oxen]Cl$_4$** (B) and complex **[(Cubipy)$_2$oxen]Cl$_4$** (C).

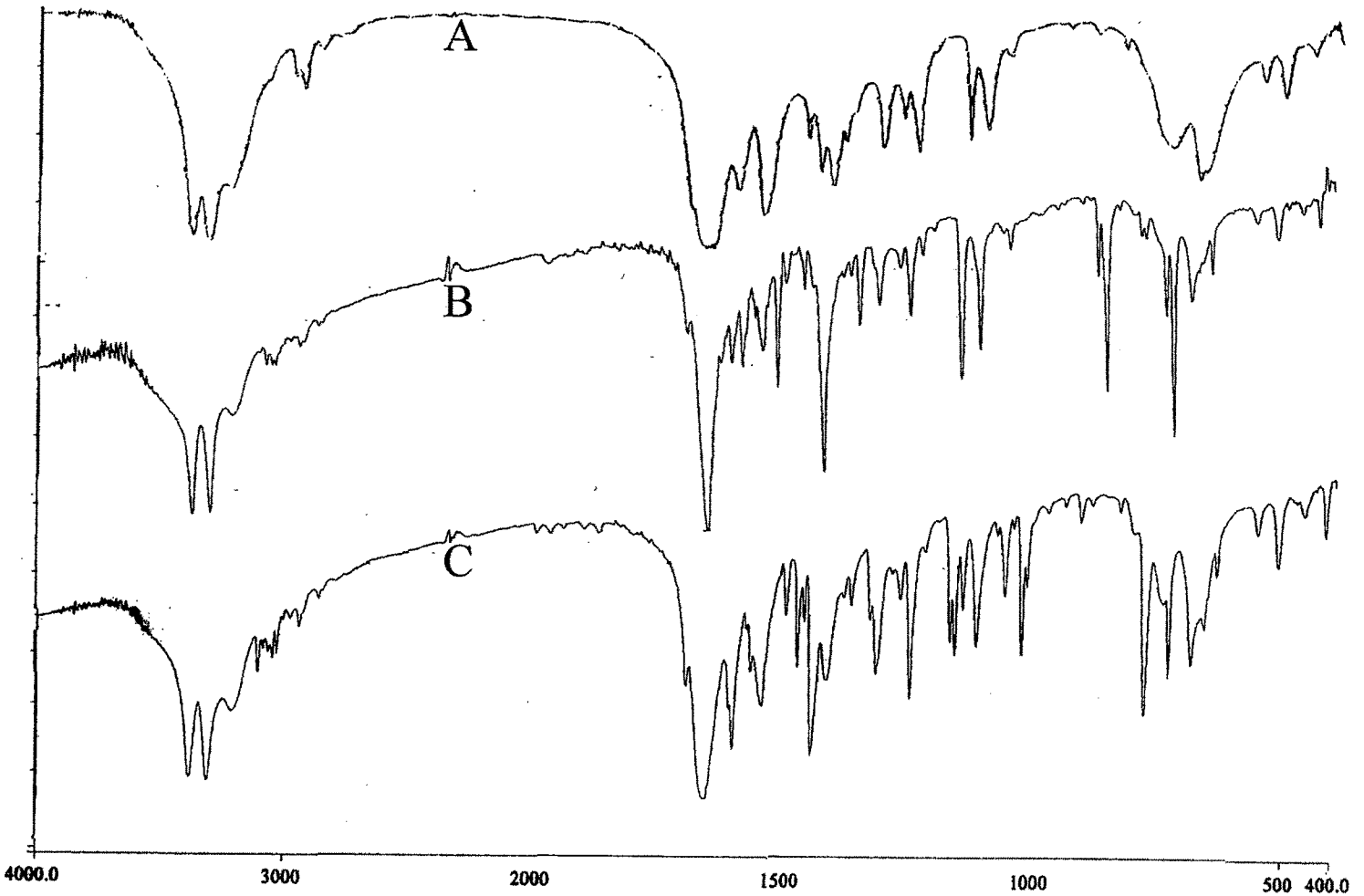

Fig.2.11 FTIR spectrum of ligand **ox2pn** (A), complex **[(Cuphen)$_2$ox2pn]Cl$_4$** (B) and complex **[(Cubipy)$_2$ox2pn]Cl$_4$** (C).

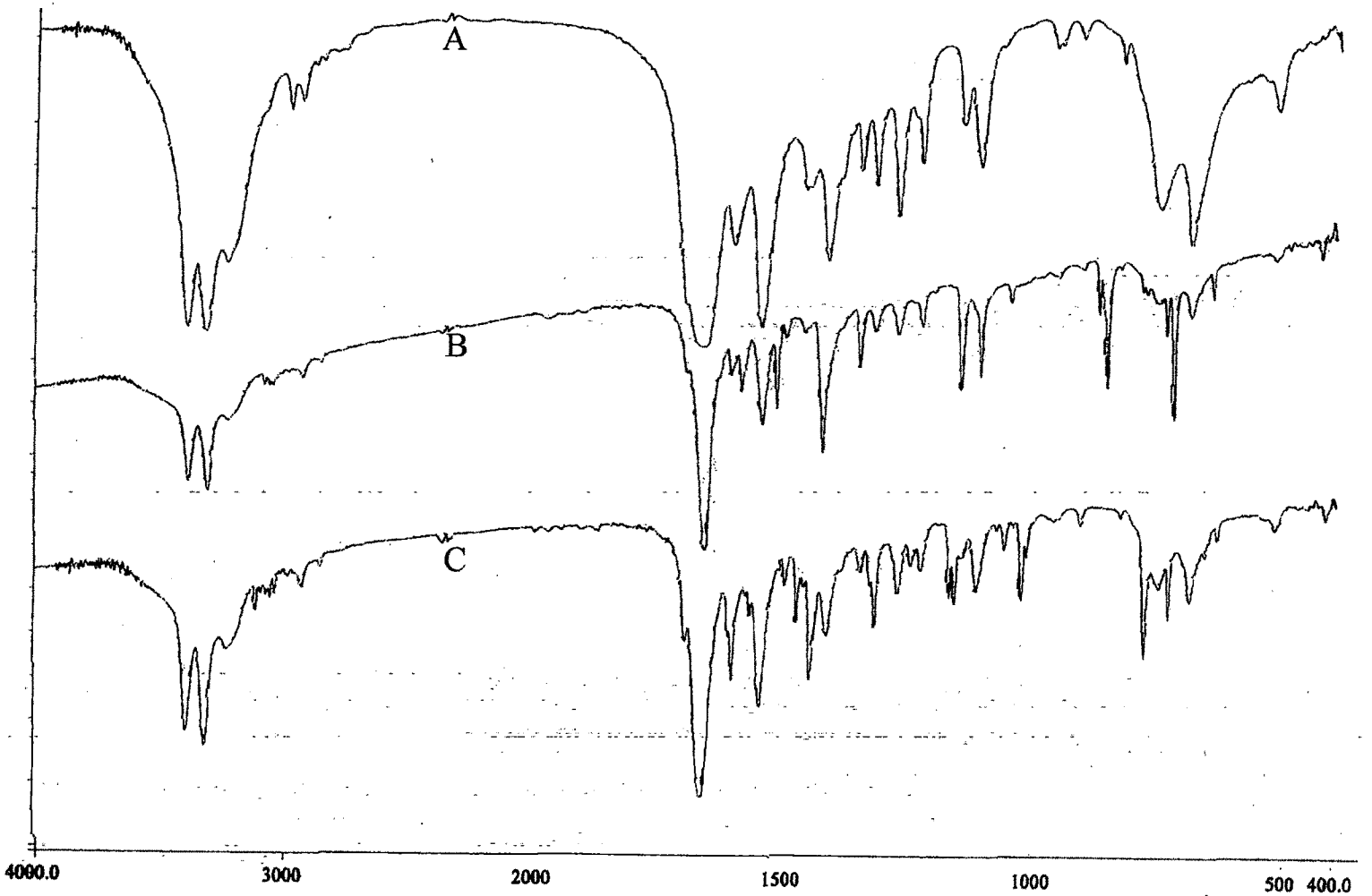

Fig 2.12 FTIR spectrum of ligand **ox3pn** (A), complex **[(Cuphen)$_2$ox3pn]Cl$_4$** (B) and complex **[(Cubipy)$_2$ox3pn]Cl$_4$** (C).

2.4 Molecular modelling of ligands and complexes

Geometry of all the three trinucleating bis-oxamide ligands was optimized by *ab initio* quantum mechanical calculations,[41] using 6-31G basis set[42,43]. The force constant and the major vibrational frequencies were calculated and compared with the experimental data. Energy of the ligands are observed to be E (RHF) = -749.994, for the ligand **oxen**, E (RHF) = -789.030 for the ligand **ox2pn** and E (RHF) = -789.014amu for the ligand **ox3pn**. It can be seen that, the >C=O bond distances in the carbonyl group are between 1.226 to 1.231Å. The -C-NH_2 (primary amide) and –C-NH- (secondary amide) bond distances are 1.334 to 1.334 Å and 1.341-1.338Å, respectively. These are shorter for a -C-N- single bond. The –C-C- bond distances in oxamide are also observed to be approximately at 1.522 to 1.524Å while the –N-H bond distances are between 1.336 to 1.341Å. The slightly longer >C=O and shorter –C-N- bond distances indicate delocalization of the π-electron density over the whole oxamide part. This resonance makes the oxamide oxygen more electron rich and hence a preferred electron donor site for coordination with copper. The plot of electron density over electrostatic potentials of ligands shows the maximum electron density located on the carbonyl oxygen as compared to amide nitrogen.

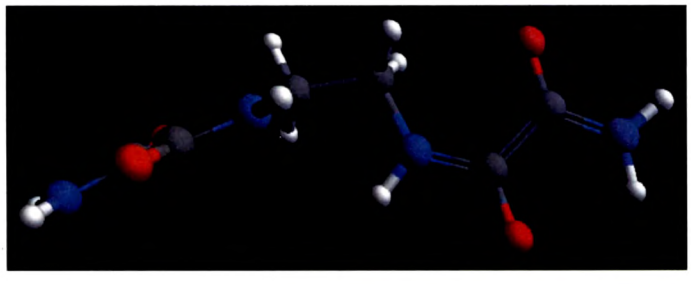

Fig.2.13 Ligand **oxen** optimized by 6-31G basis set.

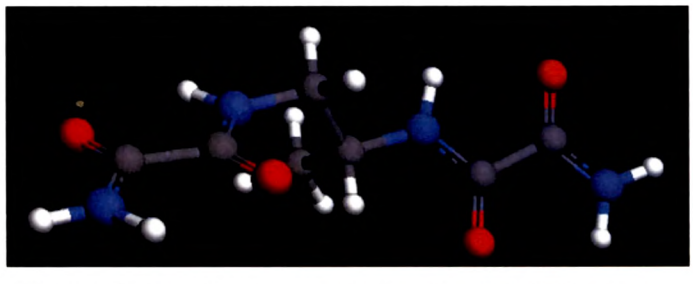

Fig.2.14 Ligand **ox2pn** optimized by 6-31G basis set.

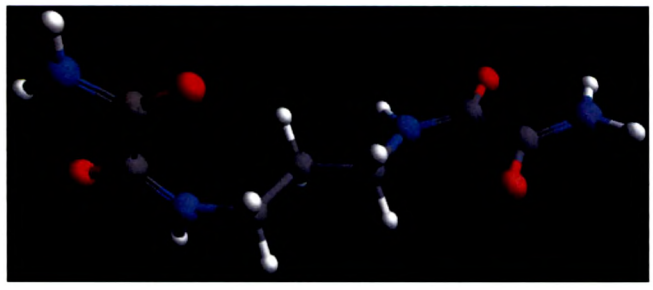

Fig.2.15 Ligand **ox2pn** optimized by 6-31G basis set.

The observation is in accord with the preference for N_2O_2 coordination environment in the present complexes as also is evidenced by the IR and ESR spectroscopy.

The geometry optimization of complexes was carried out by semi-empirical quantum mechanical calculations using Universal Force Field (UFF). [44-52] The pictorial diagrams are shown below.

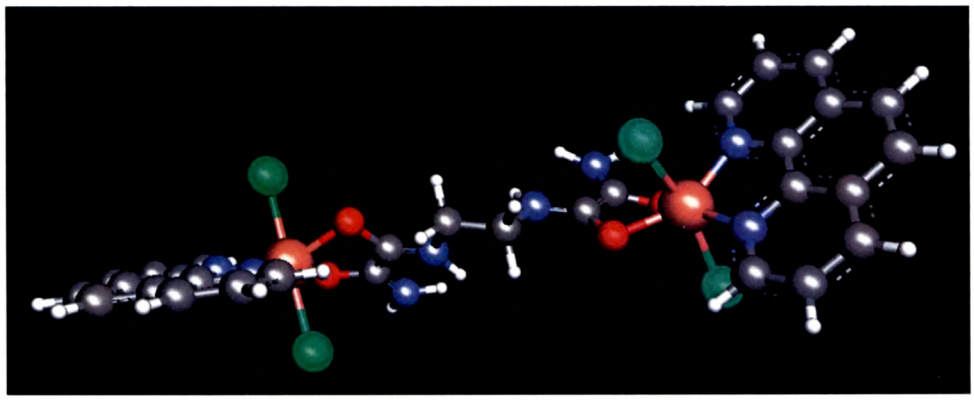

Fig.2.16 Optimized geometry of the complex **[(Cuphen)$_2$oxen]Cl$_4$**

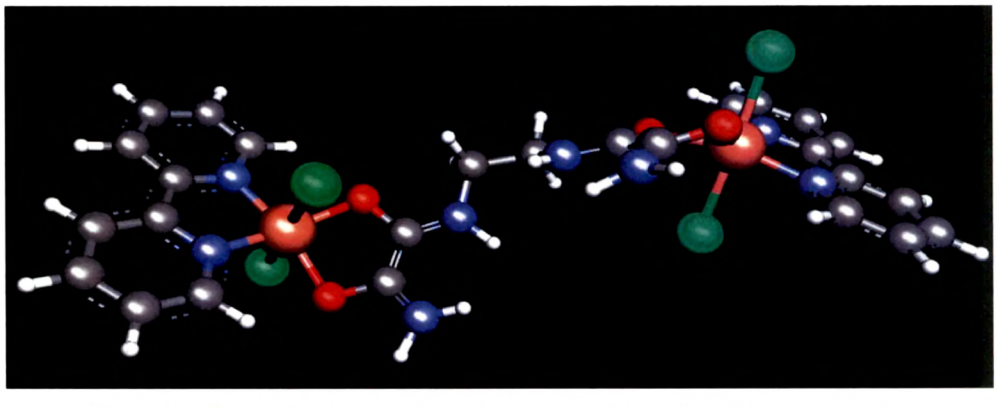

Fig.2.17 Optimized geometry of the complex **[(Cubipy)$_2$oxen]Cl$_4$**

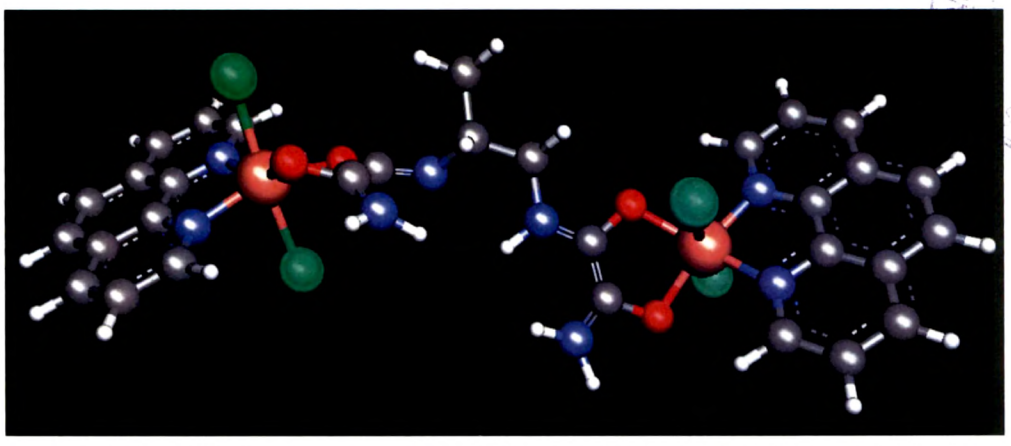

Fig.2.18 Optimized geometry of the complex **[(Cuphen)$_2$ox2pn]Cl$_4$**

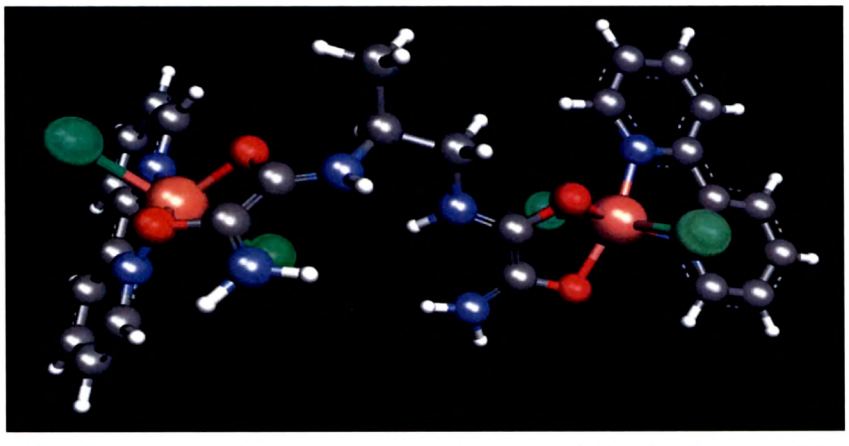

Fig.2.19 Optimized geometry of the complex **[(Cubipy)$_2$ox2pn]Cl$_4$**

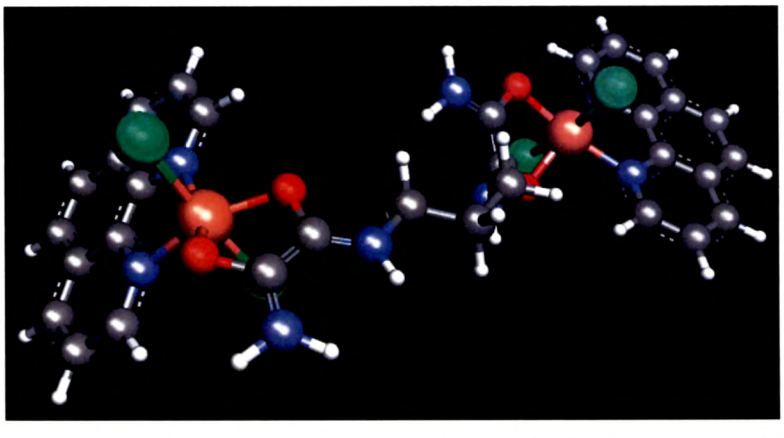

Fig.2.20 Optimized geometry of the complex **[(Cuphen)$_2$ox3pn]Cl$_4$**

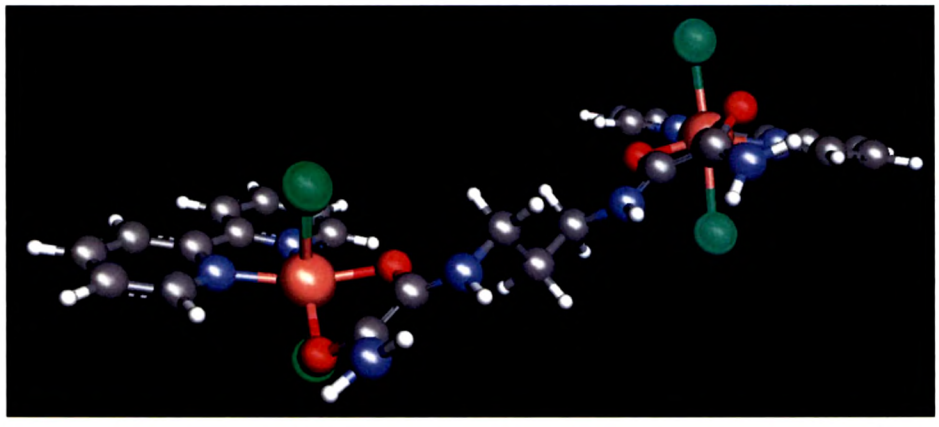

Fig.2.21 Optimized geometry of the complex **[(Cubipy)$_2$ox3pn]Cl$_4$**

The dihedral angles between the metal coordination planes have been calculated and are found to be 155, 150 and 83° respectively, in **[(Cuphen)$_2$oxen]Cl$_4$**, **[(Cubipy)$_2$ox2pn]Cl$_4$** and **[(Cubipy)$_2$ox3pn]Cl$_4$** complexes. As the dihedral angles decreases from 180 towards 90°, planarity decrease and the orthogonality of the interacting orbitals increases.

2.5 ESR spectra of Complexes

The ESR spectra of complexes **[(Cuphen)$_2$oxen]Cl$_4$**, **[(Cuphen)$_2$ox2pn]Cl$_4$** and **[(Cubipy)$_2$ox3pn]Cl$_4$** (**Fig.2.22 & 2.23**) were recorded in both powder at RT and in DMSO glass at LNT. The complexes have well resolved $g_{\parallel}$ and $g_{\perp}$ components. Hyperfine splitting was observed in DMSO solution of the complexes, from which the hyperfine coupling constants, $A_{\parallel}$ were calculated and found to be ~160cm^{-1}. This confirms the N_2O_2 coordination environment around the copper centre. Half field transitions were also observed in these complexes indicating that the two copper(II) ions are magnetically coupled in spite of having σ-bonded aliphatic bridging ligands.

Table 2.8 ESR of complex **2.6**

Complex	$A_{\parallel}$	$A_{\perp}$	$g_{\parallel}$	$g_{\perp}$
[(Cuphen)$_2$oxen]Cl$_4$	170	-------	2.12	2.07
[(Cuphen)$_2$ox2pn]Cl$_4$	155	135	2.09	2.06
[(Cubipy)$_2$ox3pn]Cl$_4$	156	-------	2.11	2.06

In DMSO.

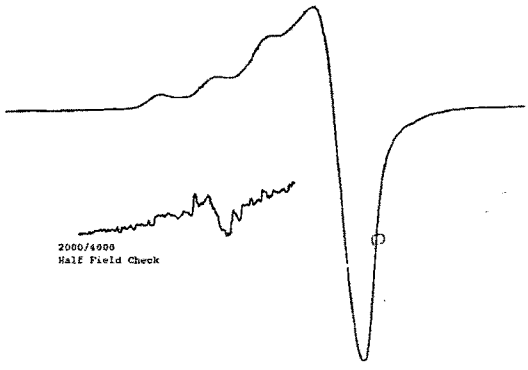

Fig.2.22

In solid state.

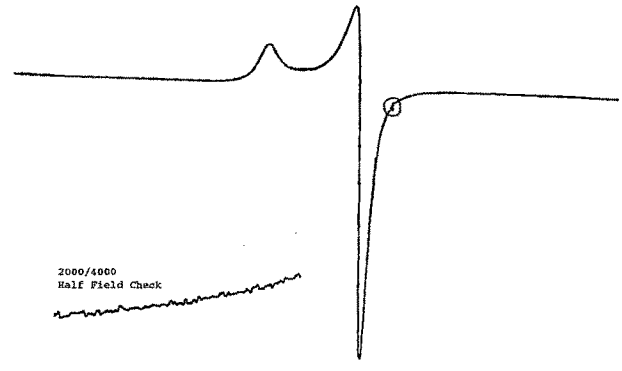

Fig.2.23

2.6 Magnetic properties of Complexes

Magnetic susceptibility of complexes **$[(Cuphen)_2oxen]Cl_4$**, **$[(Cubipy)_2ox2pn]Cl_4$**, and **$[(Cubipy)_2ox3pn]Cl_4$** was measured by Faraday method down to liquid nitrogen temperature. Having aliphatic chain in between two copper centres, all the three complexes are ferromagnetic in nature with J values 42.1, 57 and 115.3cm^{-1}, respectively. Thus, the J values follow the order **ox3pn>ox2pn>oxen**. The dihedral angles between the metal coordination planes are 155, 150 and 83. Thus change in dihedral angle directly affects the extent of spin exchange. With the deviation in the dihedral angle from planarity, i.e. 180°, the orthogonality of the interacting paramagnetic orbital increases, resulting in greater ferromagnetism. Here, it appears that, the increased number of carbon atoms in the bridging aliphatic chain leads to greater ferromagnetism. In these complexes, orthogonality decreases as the aliphatic ligands are being changed. As a result of this change ferromagnetism is induced in the complexes.

Table 2.9 Calculated values of coupling constant J and Weiss' constant θ.

Complex	θ	J (cm^{-1})	Dihedral Angle (°)
$[(Cuphen)_2oxen]Cl_4$	-10	42.1	155
$[(Cubipy)_2ox2pn]Cl_4$	10	57	150
$[(Cubipy)_2ox3pn]Cl_4$	-1	115.3	83

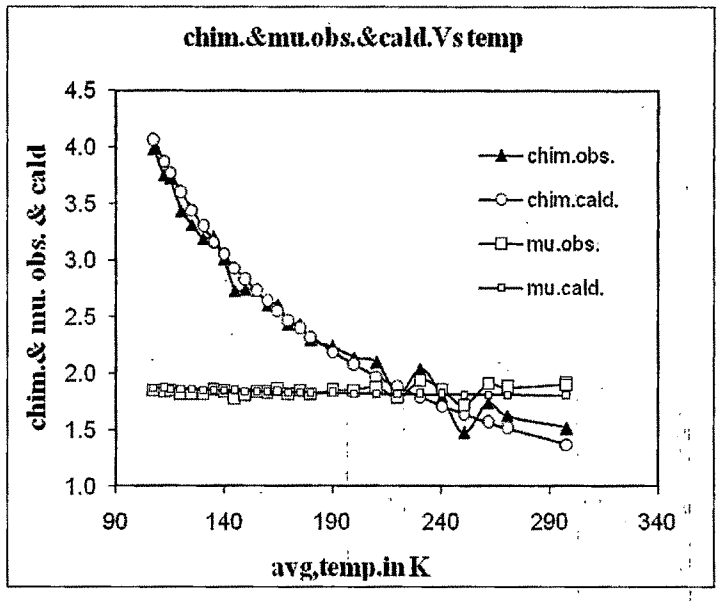

Fig.2.24 Plot of χ_M and μ (obsd. and calc.) v/s temp. of complex **[(Cuphen)$_2$oxen]Cl$_4$.**

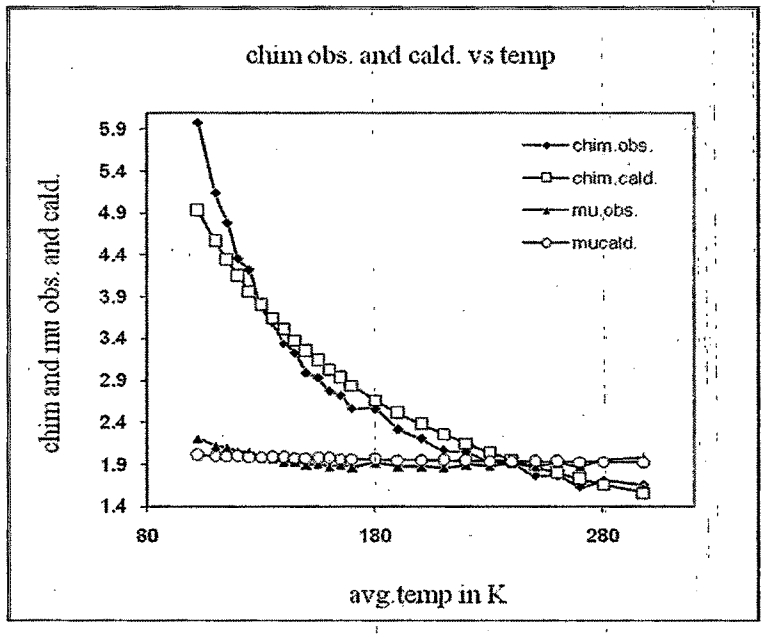

Fig.2.25 Plot of χ_M and μ (obsd. and calc.) v/s temp. in the complex **[(Cubipy)$_2$ox2pn]Cl$_4$.**

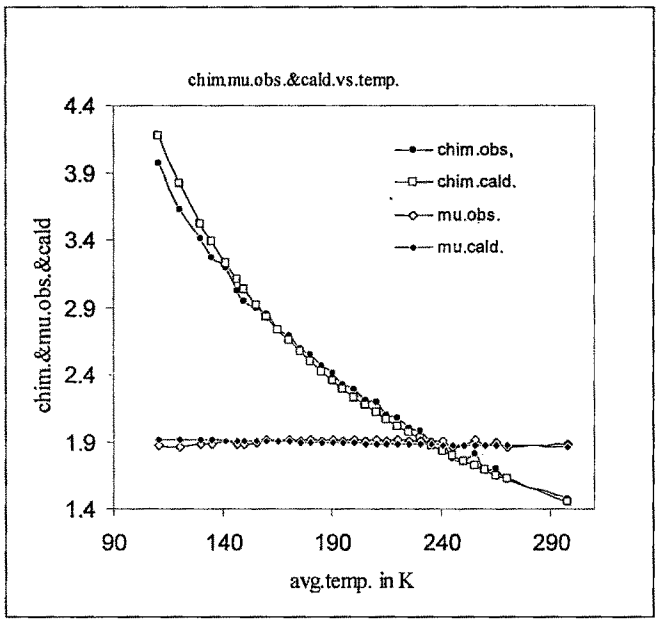

Fig.2.26 Plot of χ_M and μ (obsd. and calc.) v/s temp. in the complex **$[(Cubipy)_2ox3pn]Cl_4$.**

2.7 Cyclic Voltammetric studies

The cyclic voltammograms of the complexes have been recorded in DMSO (0.1M TBAP) solutions. The representative voltammograms are shown in Fig 2.27. All the redox potentials of complexes 1-6 are listed below (Table 2.10) with reference to $C_{p2}Fe/C_{p2}Fe^+$ couple.

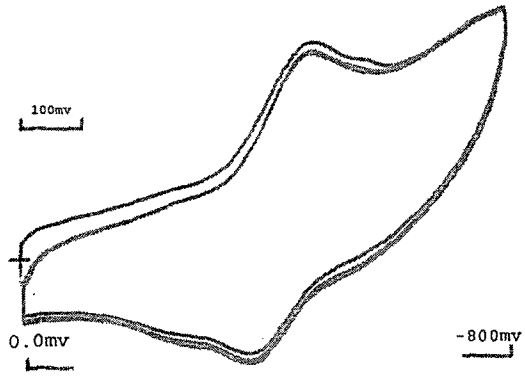

Voltammogram of Complex **$[(Cuphen)_2oxen]Cl_4$**

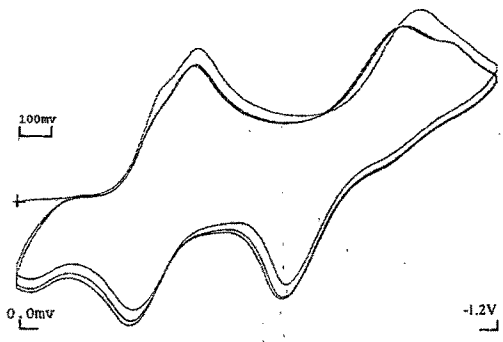

Voltammogram of Complex
[(Cuphen)$_2$ox2pn]Cl$_4$

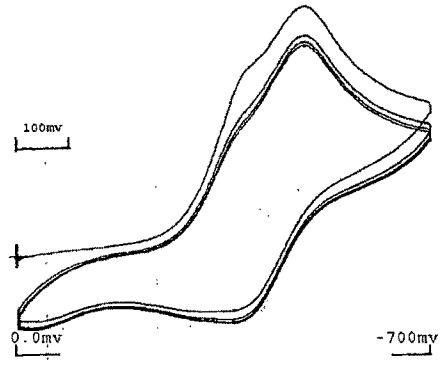

Voltammogram of Complex
[(Cuphen)$_2$ox2pn]Cl$_4$

Pt disk working electrode, Pt wire counter electrodes and Ag/AgNO$_3$ (0.1M in CH$_3$CN) as reference electrodes were used.

Fig 2.27

Table 2.10 Redox potentials of the complexes

Complex	$Epc_{(1)}$ (Volts)		$Epa_{(1)}$ (Volts)	
	$Epc_{(1)}$	$Epa_{(1)}$	$Epa_{(1)}$	$Epa_{(1)}$
[(Cuphen)$_2$oxen]Cl$_4$	-0.445	-0.345	-1.055	-0.765
(Stepwise)	-0.535	-0.245		
[(Cubipy)$_2$oxen]Cl$_4$	-0.456	-0.316	-0.916	-0.676
[(Cuphen)$_2$ox2pn]Cl$_4$	-0.386	-0.356	-1.106	-0.756
(Stepwise)	-0.496		-1.256	
[(Cubipy)$_2$ox2pn]Cl$_4$	-0.445	-0.315	-0.905	-1.015
				-0.825
[(Cuphen)$_2$ox3pn]Cl$_4$	-0.366	-0.336	-0.956	-0.796
(Stepwise)	-0.456			
[(Cubipy)$_2$ox3pn]Cl$_4$	-0.485	-0.305	-1.085	-0.715

The complexes undergo two electron, reversible or quasireversible redox to Cu^ICu^I in the range 0.0 to –0.7V. In the more negative potential region the Cu^ICu^I complex species are reduced in a single step to Cu^0Cu^0. This process is electrochemically irreversible but chemically reversible. This is indicated by the

$Cu^{I}Cu^{I} \rightarrow Cu^{I}$ process remaining intact. Because of the irreversibility of $Cu^{I}Cu^{I} \rightarrow Cu^{0}Cu^{0}$ process, a small amount of free Cu^{I} remains and gets oxidized at a less negative potential. A corresponding free $Cu^{II} \rightarrow Cu^{I}$ reduction appears in the second scan and onwards.

The complexes containing phen in complexes **$[(Cuphen)_2oxen]Cl_4$**, **$[(Cuphen)_2ox2pn]Cl_4$** and **$[(Cuphen)_2ox3pn]Cl_4$**, undergo stepwise reduction, $Cu^{II}Cu^{II} \rightarrow C^{II}Cu^{I} \rightarrow Cu^{I}Cu^{I}$. The process is more reversible and easier in the complexes containing phen than in the complexes of bipy. This is according to the expectation based on the stronger π–acidic character of phen. The stepwise redox reaffirms the presence of electronic communication between the metal centers as suggested by the presence of magnetic exchange in the complexes.

REFERENCES

(1) Li, Y.T.; Yan, C.W.; Miao, S.H., and Liao, D.Z., *Polyhedron,* 1998, **17,** 2491.

(2) Lloret, F.; Sletten, J.; Ruiz, R.; Julve, M.; Faus, J., and Verdaguer, M., *Inorg. Chem.,*1992, **31**, 778.

(3) Felthouse, T. R.; Laskowski, E. J.; Hendrickson, D. N., *Inorg. Chem.,* 1977, **5,** 1077.

(4) Julve, M.; Verdaguer, A.; Gleizes, M.; Philoche-Levisalles, Kahn, O., *Inorg. Chem.,*1984, **23,** 3808.

(5) Santana, M. D.; Garcia, G.; Julve, M.; Lloret, F.; Perez, J.; Liu, M.; Sanz, F.; Cano, J., and Lopez, G., *Inorg. Chem.,* 2004, **43**, 2132.

(6) Messori, L.; Shaw, J.; Camalli, M.; Murza, P., and Marcon, G., *Inorg. Chem.,* 2003, **42**, 6166.

(7) Kou, H. Z.; Zhou, B. C.; Gao, S., and Wang, R. J., *Angew. Chem. Int. Ed.,* 2003, **42**, 3288.

(8) Zhang, C.; Sun, J.; Kong X., and Zhao, C., *Acta Cryst.,* 1999, **C55,** 873.

(9) Ruiz, R.; Surville-Berland, C.; Aukauloo, A.; Anxolabehere-Mallart, E.; Journaux Y.; Cano, J., and Muffoz, M. C., *J. Chem. Soc. Dalton Trans,* 1997, 745.

(10) Cervera, B.; Jose, L.; Maria, S.; Ibanez, J.; Vila, G.; Loret, F. L.; Julve, M.; Ruiz, R.; Ottenwaelder, X.; Aukauloo A.; Poussereau, S.; Journaux, Y., and Munoz, M. C., *J. Chem. Soc. Dalton Trans.,* 1998, 781.

(11) Collins, T. F., *Acc. Chem. Res.,* 1994, **27,** 279 and refs. therein.

(12) Nag, K., and Chakravorty, A., *Coord. Chem. Rev.,* 1980, **33,** 87.

(13) Sigel, H., and Martin, R. B., *Chem. Rev.,* 1982, **82,** 385.

(14) (a) Bour, J. J.; Birker, P. J. M. W. L., and Steggerda, J. J., *Inorg. Chem.,* 1971, **10,** 1202. (b) Soto, J.; Manez, R. M.; Paya, J.; Lloret, F., and Julve, M., *Transition Met. Chem.,* 1993, **18,** 69. (c) Fritsky, I. O.; Kozlowski, H.; Kanderal, O. M.; Haukka, M.; Kozlowska, J. S.; Kontecka, E. G., and Meyer, F., *J. Chem. Soc., Chem. Commun.,* 2006, 4125.

(15) Zhang, C.; Sun, J.; Kong, X., and Zhao C., *Acta Cryst.,* 1999, **C55,** 873.

(16) Costa, R.; Garcia, A.; Ribas, J.; Mallah, T.; Journaux, Y.; Sletten, J.; Solans, X.; Rodriguez, V., *Inorg. Chem.,* 1993, **32,** 3733.

(17) Costa, R.; Garcia, A.; Sanchez, R.; Ribas, J.; Solans, X.; Rodriguez, V., *Polyhedron,* 1993, **12,** 2697.

(18) Tercero, J.; Diaz, C.; Ribas, J.; Mahia, J.; Maestro, M. A., *Inorg. Chem.*, 2002, **41,** 5373.

(19) Wang, Q. L.; Liao, D. Z.; Yan, S. P.; Jiang, Z.H.; Cheng, P., *Chin. J. Chem.* 2002, **20,** 1249.

(20) Tercero, J.; Diaz, C.; El Fallah, M.S.; Ribas, J.; Solans, X.; Maestro, M.A.; Mahia, J., *Inorg. Chem.*, 2001, **40,** 3077.

(21) Lloret, F.; Sletten J.; Ruiz, R.; Julve, M.; Faus, J., and Verdaguer, M., *Inorg. Chem.*, 1992, **31,** 778.

(22) Ojima, H.; No K., *Ryoiki,* 1972, **26,** 70.

(23) Ojima, H., *Bull. Aichi Univ. Educ.*, (Natural Sci. Sect.), 1971, **11,** 103.

(24) (a) Lloret F.; Jaurnaux, Y., and Julve, M., *Inorg. Chem.*, 1990, **29,** 3967. (b) Tang, J.; Si, S.; Wang, L.; Liao, D.; Jiang, Z.; Yan, S.; Cheng, P., and Liu, X., *Inorg. Chim. Acta.*, 2003, **343,** 288.

(25) (a) *J. Chem. Soc., Dalton Trans.*, 1992, 95. (b) *Inorg. Chim. Acta.* 2008, **361,** 3847. (c) Patel, K. B.; Patel, M. N. *J. of Chem. Sci.*, 2008, **97, 5-6,** 535.

(26) (a) Masuda, H.; Sgineri, T.; Konzuma, T.; Odani, A. and Yamauchi, O. *Bull. of Chem. Soc. of Jpn.* 1992, **65,** 786. (b) Higham, C. S.; Dawling, D. P.; Shaw, J. L.; Cetin, A.; Ziegler, C. J. and Forrell, J. R. *Tetrahedron Letters,* 2006, **47,** 4419.

(27) (a) Ojima, H., and Nonoyama, K., *Bull. Aichi Univ. Educ.*, 1986, **35,** 75. (b) Ojima, H., and Nonoyama, K., *Z. anorg. Allgem. Chem.*, 1977, **429,** 275. (c) Tercero, J.; diaz, C; Ribas, J.; Mahia, J.; Maestro, M., and Solans, X., *J. Chem. Soc. Dalton Trans,* 2002, 2040.

(28) Cervera, B.; Sanz, J. L.; Inanez, M. J.; Vila, G.; Loret, F. L.; Julve, M.; Ruiz, R.; Ottenwaeldet, X.; Aukauloo, A.; Poussereau, S.; Jounaux, Y., and Munoz, M. C., *J. Chem. Soc. Dalton Trans.* 1998, 781.

(29) Nokoyama, K.; Ojima, H., and Nonoyama, M., *Inorg. Chim Acta,* 1976, **20,** 127.

(30) Ruiz. R.; Faus. J.; Lloret. R.; Julve, M., and Journaux, Y., *Coord. Chem. Rev.*, 1999, **193,** 1069.

(31) Ojima, H., and Nonoyama, K., *Coord. Chem. Rev.*, 1988, **92,** 85.

(32) Journaux Y.; Sletten, J.; Kahn, O., *Inorg. Chem.*, 1985, **24,** 4063.

(33) Ruffer, T.; Brauer, B.; Powell, A. K.; Hewitt, I., and Salvan, G., *Inorg. Chim. Acta.*, 2007, **360,** 3475.

(34) Ojima, H.; Ryoiki, K. N., 1972, **26,** 70. And Ojima, H., *Bull Aichi Univ. Educ.,* 11 (Natural Sci. Sect.) 1971, 103.

(35) Nonoyama, K.; Ojima, H., and Nonoyama, M., *Inorg. Chim. Acta,* 1976, **20,** 127.

(36) Ojima, H., and Nonoyama, K., 32nd Nat. Meet of Chem. Soc. Jpn., Proceedings 1, *Chemical Society of Japan,* 1975, p.536.

(37) Lloret, F.; Sletten, J.; Ruiz, R.; Julve, M.; Faus, J., and Verdaguer, M., *Inorg. Chem.,* 1992, **31,** 778.

(38) Sigel, H., *Inorg. Chem.,* 1975, **14,** 1535.

(39) Nair, M. S.; Santappa, M., and Natarajan, P., *Ind. J. Chem.,* 1980, **19a,** 672.

(40) Ojima, H., and Nonoyama, K., *Z. anorg. Allgem. Chem.,* 1973, **401,** 195.

(41) Schmidt, M.W.; Baldridge, K. K.; Boatz, J. A.; Elbert, S. T.; Gordon, M. S.; Jensen, Montgomery, J. A. *J. Comput Chem.* 1993, **14,** 1347.

(42) Ditchfield, R.; Hehre, W. J.; Pople, J. A.; *J. Chem. Phys.* 1971, **54,** 724.

(43) Hehre, W. J.; Ditchfield, R.; Pople, J. A.; *J. Chem. Phys.* 1972, **56,** 2257.

(44) Rassolov, V. A.; Pople, J. A.; Ratner, M. A.; Windus, T. L.; *J. Chem. Phys.* 1998, **109,** 1223.

(45) Casewit, C. J., Colwell, K. S., and Rappe', A. K., *J. Am. Chem. Soc.,* 1992, **114,** 10035.

(46) Casewit, C. J., Colwell, K. S., and Rappe', A. K., *J. Am. Chem. Soc.,* 1992, **114,** 10046.

(47) Rappe', A. K. and Goddard, W. A., *J. Phy. Chem.,* 1991, **95,** 3358.

(48) Rappe', A. K., Colwell, K. S., and Casewit, C. J., *Inorg. Chem.* 1993, **32,** 3438.

(49) Thompson, M. A., Zerner M. C. *J. Am. Chem. Soc.,* 1991, **113,** 8210.

(50) Thompson, Mark A.; Glendening, Eric D. and Feller, David *J. Phys. Chem. 1994,* 10465.

(51) Thompson, Mark A. and Schenter, Gregory K. *J. Phys. Chem.* 1995, **99,** 6374.

(52) Thompson, Mark A.; *J. Phys. Chem.* 1996, **100,** 14492.